

Stabilizing New Morphologies by Blending Homopolymer with Block Copolymer

M. W. Matsen

Department of Chemical Engineering and Materials Science, University of Minnesota, Minneapolis, Minnesota 55455
(Received 15 November 1994)

We examine weakly segregated blends of AB diblock copolymer and A homopolymer using self-consistent field theory. The addition of homopolymer to a diblock melt is found to stabilize new ordered morphologies: close-packed spheres, hexagonally perforated lamellae, and bicontinuous cubic ($Q_{Pn\bar{3}m}$ and $Q_{Ia\bar{3}d}$) phases. We find highly swollen phases that we associate with spherical, cylindrical, and lamellar micellar regions, and with disordered struts.

PACS numbers: 61.20.Gy, 61.25.Hq, 64.80.Gd

Molecular self-assembly is a phenomenon that occurs in lipid [1–4], surfactant [5–7], liquid crystal [8,9], block copolymer [10,11], and numerous other “soft material” systems. In many cases, they form disordered structures such as micelles [1,5,6], vesicles [2], sponge phases [5], and bicontinuous microemulsions [6]. However, they can also form ordered structures with long coherence lengths [8]. A remarkable feature is that these varied systems tend to favor structures of the same symmetries, suggesting a kind of universality. Commonly, the ordered structures are monocontinuous arrangements of lamellar, cylindrical, or spherical micellar units [1,3–5,7,8,10,11], but occasionally they are intriguing bicontinuous cubic ones possessing $Im\bar{3}m$, $Pn\bar{3}m$, and $Ia\bar{3}d$ symmetries. Lipid-water mixtures [1,3,4] are well known for exhibiting the latter structures, which also occur in numerous other systems [5,7,10,11] including even thermotropic liquid crystals [9]. Observations [3,12] of these bicontinuous structures in biological systems are now stimulating interest regarding the role of ordering transitions and metabolic functions [13].

Of all the systems exhibiting self-assembly, block copolymers offer perhaps the best opportunity for a systematic study due to the extreme latitude in experimental ability to control the properties and architecture of these molecules. Furthermore, theoretical techniques for calculating their behavior are sufficiently advanced to deal with the complex symmetries. Accordingly, this class of materials provides a unique opportunity to advance the general understanding of self-assembly. In order to do so, it will be necessary to go beyond pure (i.e., single-component) copolymer melts and consider blends that are more closely analogous to the multicomponent amphiphilic systems. A model system for doing so is the binary blend of AB diblock copolymer with A homopolymer. We will find that this system exhibits many of the features found in lipid-water mixtures with additional ordered microstructures, macrophase separation, and micellar regions.

Because diblock copolymers form a rich variety of structures on their own, they are most often studied as one-component systems [10,11,14]. The physics of these systems is well understood [10]. Immiscibility between A and B monomers drives the formation of a microstructure.

As this occurs, incompressibility of the melt requires the overall monomer density to remain uniform, which can only be accomplished if the molecules stretch. The competition between interfacial tension where A - and B -monomer regions meet and tension in the stretched polymers determines the length scale of the structure. Symmetric A and B blocks will result in flat interfaces producing the lamellar (L) microstructure. However, if a sufficient asymmetry exists between the blocks, then the interfaces will curve producing, for example, cylinders or spheres. The arrangement of these units is largely determined by packing constraints. Those that tend to fill space well are favored since they require only small deformations in the units in order to maintain a uniform monomer density. For the cylindrical units, the favored arrangement is hexagonal (H), and for the spheres it is body-centered cubic ($Q_{Im\bar{3}m}$). There are several more elaborate structures which may also occur. They include two bicontinuous cubic phases, $Q_{Pn\bar{3}m}$ and $Q_{Ia\bar{3}d}$, commonly referred to as double diamond and gyroid, respectively, and a hexagonally perforated lamellar (HPL) phase often referred to as catenoid lamellar. The latter is much like the L phase except that the thin minority-component lamellae are perforated. The perforations are arranged hexagonally within the layer and staggered between adjacent layers. The two bicontinuous phases are similar in that the minority component forms two interweaving lattices separated by a majority-component matrix. The vertices of the $Q_{Ia\bar{3}d}$ and $Q_{Pn\bar{3}m}$ lattices are threefold and fourfold coordinated, respectively. We note that uncertainty exists regarding the stability of the $Q_{Pn\bar{3}m}$ phase in copolymer melts [10,11,15].

The addition of a homopolymer to the copolymer melt produces a system [16–21] more analogous to the amphiphile-water one, where homopolymer plays the role of water. Adding homopolymer to the melt not only leads to regions of two-phase coexistence which cannot exist in a single-component system, but it also affects the relative stability of the various morphologies. A way in which the homopolymer accomplishes the latter is by filling the spaces that otherwise would have to be filled by highly stretched copolymers. Because this will affect

the different microstructures to different degrees, it may bring about new equilibrium phases. For example, there are reasons to suspect that homopolymer could cause the spheres in the $Q_{1m\bar{3}m}$ phase to reorder into a close-packed arrangement [22,23] or perhaps a simple cubic one [16].

In this Letter, we consider the phase behavior of weakly segregated blends [24] using self-consistent field theory (SCFT) [25] and examining all the phases discussed above. The blends consist of n_c AB diblock copolymers of polymerization index N and n_h A homopolymers of index αN . We assume a fixed monomer density ρ_0 such that the melt is incompressible. Each polymer is parametrized with a variable s that increases continuously along its length so that equal increments in s correspond to equal volumes of polymer. For a homopolymer $0 \leq s \leq \alpha$ and for a copolymer $0 \leq s \leq f$ along the A block and $f \leq s \leq 1$ along the B block. These parametrizations allow us to define functions, $\mathbf{r}_{c,l}(s)$ for the l th copolymer and $\mathbf{r}_{h,l}(s)$ for the l th homopolymer, to specify their configuration.

The original formulation of the SCFT for multicomponent polymer systems [26] used the canonical ensemble. Here we reformulate it in the grand canonical ensemble starting from the grand partition function,

$$Z = \sum_{n_c=0}^{\infty} \sum_{n_h=0}^{\infty} \frac{z_0^{n_c} (z z_0)^{n_h}}{n_c! n_h!} \int \prod_{l=1}^{n_c} \tilde{\mathcal{D}}\mathbf{r}_{c,l} \prod_{l=1}^{n_h} \tilde{\mathcal{D}}\mathbf{r}_{h,l} \times \delta[1 - \hat{\Phi}_A - \hat{\Phi}_B] \exp\left\{-\chi \rho_0 \int d\mathbf{r} \hat{\Phi}_A \hat{\Phi}_B\right\}, \quad (1)$$

where $z = \exp(\mu/k_B T)$ and μ is the chemical potential for the homopolymer to within an additive constant determined by z_0 . To simplify the formulas that follow, we set $z_0 = \rho_0/N$. The chemical potential for the copolymer has been set to zero, which is permitted due to the incompressibility enforced by the delta functional in Eq. (1). The factor $n_c!$ accounts for the indistinguishability of copolymer molecules, and $n_h!$ does the same for homopolymers. Tildes indicate that the functional integrals are weighted by $P[\mathbf{r}_{c,l}; 0, 1]$ for copolymers and by $P[\mathbf{r}_{h,l}; 0, \alpha]$ for homopolymers, where

$$P[\mathbf{r}; s_1, s_2] \propto \exp\left\{-\frac{3}{2Na^2} \int_{s_1}^{s_2} ds \left| \frac{d}{ds} \mathbf{r}(s) \right|^2\right\}.$$

The statistical segment length a is assumed to be the same for A and B monomers. The dimensionless A -monomer-density operator in Eq. (1) is given by

$$\hat{\Phi}_A(\mathbf{r}) = \frac{N}{\rho_0} \sum_{l=1}^{n_c} \int_0^f ds \delta(\mathbf{r} - \mathbf{r}_{c,l}(s)) + \frac{N}{\rho_0} \sum_{l=1}^{n_h} \int_0^\alpha ds \delta(\mathbf{r} - \mathbf{r}_{h,l}(s)),$$

where the first sum is over copolymer molecules and the second is over homopolymers. The expression for $\hat{\Phi}_B(\mathbf{r})$ is similar except that it has no homopolymer

contribution. The Flory-Huggins parameter χ measures the incompatibility between A and B monomers.

We take several steps to make Eq. (1) more manageable. First, we insert a functional integral, $1 = \int \mathcal{D}\Phi_A \delta[\Phi_A - \hat{\Phi}_A]$, which permits the replacement of the operator $\hat{\Phi}_A$ by the function Φ_A . After doing the same for $\hat{\Phi}_B$, the delta functionals are replaced by standard integral representations [26]. Finally, using $\sum_n x^n/n! = \exp(x)$ to evaluate the two summations, we obtain

$$Z = \mathcal{N} \int \mathcal{D}\Phi_A \mathcal{D}W_A \mathcal{D}\Phi_B \mathcal{D}W_B \mathcal{D}\Xi \exp\{-F/k_B T\}, \quad (2)$$

where \mathcal{N} is a normalization constant,

$$NF/k_B T \rho_0 \equiv -\mathcal{Q}_c - z \mathcal{Q}_h + \int d\mathbf{r} [\chi N \Phi_A \Phi_B - W_A \Phi_A - W_B \Phi_B - \Xi(1 - \Phi_A - \Phi_B)], \quad (3)$$

$$\mathcal{Q}_c \equiv \int \tilde{\mathcal{D}}\mathbf{r}_c \exp\left\{-\int_0^f ds W_A(\mathbf{r}_c) - \int_f^1 ds W_B(\mathbf{r}_c)\right\},$$

$$\mathcal{Q}_h \equiv \int \tilde{\mathcal{D}}\mathbf{r}_h \exp\left\{-\int_0^\alpha ds W_A(\mathbf{r}_h)\right\}.$$

The functional $F[\Phi_A, W_A, \Phi_B, W_B, \Xi]$ in Eq. (3) can be evaluated, but the functional integral in Eq. (2) cannot. In the SCFT [26], one approximates this integral by the extremum of the integrand. Thus, the free energy $-k_B T \ln Z$ is approximated by $F[\phi_A, w_A, \phi_B, w_B, \xi]$, where ϕ_A, w_A, ϕ_B, w_B , and ξ are the functions for which F attains its minimum. Requiring variations in F with respect to each of its five functions to be zero, we obtain

$$\phi_A = \frac{\mathcal{D}\mathcal{Q}_c}{\mathcal{D}W_A} + z \frac{\mathcal{D}\mathcal{Q}_h}{\mathcal{D}W_A}, \quad (4)$$

$$\phi_B = \frac{\mathcal{D}\mathcal{Q}_c}{\mathcal{D}W_B}, \quad (5)$$

$$\phi_A(\mathbf{r}) + \phi_B(\mathbf{r}) = 1, \quad (6)$$

$$w_A(\mathbf{r}) = \chi N \phi_B(\mathbf{r}) + \xi(\mathbf{r}), \quad (7)$$

$$w_B(\mathbf{r}) = \chi N \phi_A(\mathbf{r}) + \xi(\mathbf{r}). \quad (8)$$

The interpretation of these equations is straightforward once it is recognized that $\mathcal{Q}_c[w_A, w_B]$ is the partition function for a copolymer with A and B monomers subject to fields $w_A(\mathbf{r})$ and $w_B(\mathbf{r})$, respectively, and that $\mathcal{Q}_h[w_A]$ is the same but for a homopolymer. Equations (4) and (5) identify $\phi_A(\mathbf{r})$ and $\phi_B(\mathbf{r})$ as average A - and B -monomer densities, Eq. (6) is the incompressibility constraint, and Eqs. (7) and (8) are the self-consistent equations that the fields must satisfy.

To solve the partition function for the diblock copolymer, one writes it as $\mathcal{Q}_c = \int d\mathbf{r} q_c(\mathbf{r}, 1)$, where $q_c(\mathbf{r}, s)$ is an end-segment distribution function. Specifically, it is

the partition function for the segment of chain from 0 to s subject to the constraint $\mathbf{r}_{c,i}(s) = \mathbf{r}$, and it satisfies

$$\frac{\partial q_c}{\partial s} = \begin{cases} \frac{1}{6} Na^2 \nabla^2 q_c - w_A(\mathbf{r}) q_c & \text{if } s < f, \\ \frac{1}{6} Na^2 \nabla^2 q_c - w_B(\mathbf{r}) q_c & \text{if } f < s, \end{cases} \quad (9)$$

with the initial condition $q_c(\mathbf{r}, 0) = 1$ [25]. Because the two ends of the copolymer are distinct, a second distribution function $q_c^\dagger(\mathbf{r}, s)$ is defined for the other portion of the chain (s to 1) again subject to the same constraint. It satisfies $q_c^\dagger(\mathbf{r}, 1) = 1$, and Eq. (9) with the right-hand side multiplied by -1 . For the homopolymer, things are simpler. Its partition function is $\mathcal{Q}_h = \int d\mathbf{r} q_h(\mathbf{r}, \alpha)$ where $q_h(\mathbf{r}, 0) = 1$ and

$$\frac{\partial q_h}{\partial s} = \frac{1}{6} Na^2 \nabla^2 q_h - w_A(\mathbf{r}) q_h.$$

Because both ends of a homopolymer are identical, a second distribution function is not needed.

In terms of the above end-segment distribution functions, the A -monomer density, Eq. (4), can be written

$$\phi_A(\mathbf{r}) = \int_0^f ds q_c(\mathbf{r}, s) q_c^\dagger(\mathbf{r}, s) + z \int_0^\alpha ds q_h(\mathbf{r}, s) q_h(\mathbf{r}, \alpha - s).$$

The expression for $\phi_B(\mathbf{r})$ is similar except there is no homopolymer contribution. These expressions satisfy Eqs. (4) and (5). To satisfy the remaining three Eqs. (6)–(8), we adjust $w_A(\mathbf{r})$, $w_B(\mathbf{r})$, and $\xi(\mathbf{r})$. This is done numerically using the method described in Ref. [14]. There will, in general, be multiple solutions, each corresponding to its own phase with a free energy F given by

$$NF/k_B T \rho_0 = -\mathcal{Q}_c - z \mathcal{Q}_h - \int d\mathbf{r} [\chi N \phi_A \phi_B + \xi].$$

By comparing F for different structures, a phase diagram can be constructed. Although our calculations are performed in the grand-canonical ensemble, we plot our results in terms of the canonical coordinates χN , f , α , and ϕ , where the latter is the homopolymer volume fraction (i.e., the conjugate to μ). Below, we discuss the case in Fig. 1 for $\chi N = 11$ and $\alpha = 2/3$. Because we are dealing with a two-component blend, in general, all one-phase regions will be separated by two-phase coexistence regions. In many instances, these biphasic regions are so small that they are not visible on the scale of Fig. 1.

The theoretical phase diagram for the pure diblock (i.e., $\phi = 0$) is presented in Ref. [14], and at $\chi N = 11$, only the L, H, and $Q_{1m\bar{3}m}$ ordered phases are stable. We find that the homopolymer produces additional morphologies. For instance, addition of the homopolymer to the matrix of the $Q_{1m\bar{3}m}$ phase can cause the rearrangement of the spheres into a close-packed configuration, the close-packed sphere (CPS) phase [22]. Furthermore, the homopolymer causes the $Q_{1a\bar{3}d}$ phase to emerge between the L and H ones in much the same way as it does when

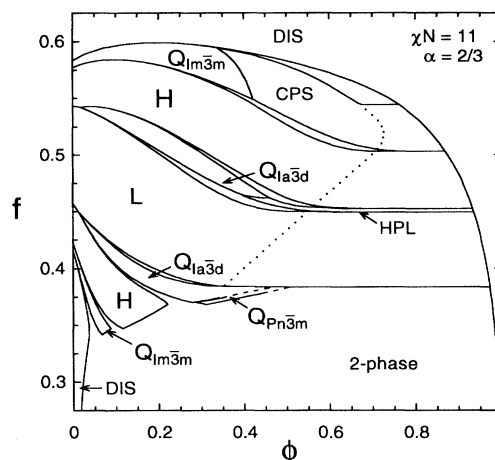


FIG. 1. Phase diagram for blends of AB diblock and A homopolymer plotted in terms of the homopolymer volume fraction ϕ and the A -monomer fraction of the copolymer f with χN and α held fixed. Dashed lines are extrapolated phase boundaries, and the dotted line shows (hypothetically) where swollen microphases might disorder into a micellar region. For clarity, only the largest biphasic region is labeled.

χN increases [14]. Increasing ϕ further causes the $Q_{1a\bar{3}d}$ phase to switch to either the HPL or the $Q_{pn\bar{3}m}$ phase, depending on whether the homopolymer is added to the matrix or the minority-component lattices. In the latter case, numerical limitations prevented us from fully determining the phase boundaries of the $Q_{pn\bar{3}m}$ phase, but we have results suggesting that it completely separates the $Q_{1a\bar{3}d}$ phase from the homopolymer-rich disordered (DIS) phase as indicated with dashed lines in Fig. 1. Notably, this is the same arrangement of the bicontinuous cubic phases found in lipid-water mixtures [3,4].

For the HPL and the CPS phases, there is a question of how the lamellae and the spheres actually pack. In the regions where we can evaluate free energy differences to a part in 10^6 , we find the HPL phase favors the $abab\dots$ stacking of lamellae over the $abcabc\dots$ one, and the CPS phase favors the hcp arrangement of spheres over the fcc one. In real systems, we expect such small energy differences to be irrelevant in comparison to nonequilibrium effects.

As observed experimentally [19], we find that microstructures can only accommodate a small amount of minority-component homopolymer before macrophase separation occurs, but they can accommodate large quantities of majority-component homopolymer. Within the present mean-field theory, majority-component homopolymer swells the microstructures eventually leading to continuous unbinding transitions. In Fig. 1, the unbinding transitions occur between the L, HPL, H, and CPS phases and the DIS phase in the interval $0.383 < f < 0.544$. It is clear that extremely swollen microstructures will be disordered by fluctuations not

considered within the present theory. However, this should occur in a predictable way. Fluctuations will form a micellar region between some weak first-order transition [23] (shown schematically with a dotted line in Fig. 1) and the unbinding transition. The mean-field unbinding transition will become the critical micelle concentration (CMC) calculated in Ref. [27], and what were transitions between the L, HPL, H, and CPS microstructures will become dividing lines between different micellar regions. None of these lines will remain as thermodynamic transitions [28], and, thus, the micellar region will become part of the DIS phase.

Naturally, we expect fluctuations to cause the swollen L, H, and CPS phases to disorder into lamellar, cylindrical, and spherical micellar regions, respectively [16–18]. What happens to the swollen HPL phase is less obvious. When the HPL phase swells we find that not only does the spacing between minority-component lamellae increase, but so does the size of the perforations. Eventually, the minority-component lamellae resemble honeycomb lattices, which we note are threefold coordinate as are the two lattices comprising the $Q_{Ia\bar{3}d}$ phase [11]. So when the swollen HPL phase disorders, we speculate that it will form a random network of struts where the majority of the vertices are threefold coordinated.

The phase behavior we have described agrees well with available experimental results, if one keeps in mind that small modifications to Fig. 1 can be achieved by changing χN and α . For $f \approx 0.45$, we have behavior similar to that reported by Disko *et al.* [20]. With the addition of the homopolymer, their system goes from the L phase to a L + HPL biphasic region, to the HPL phase, and, finally, to disordered struts as speculated above. Similar evidence for the HPL phase and disorder struts has been reported for blends of starblock copolymer and homopolymer [21]. Winey, Thomas, and Fetters [19] have reported the sequence L to L + H to $Q_{Pn\bar{3}m}$ to H with increasing ϕ . Based on our results, we believe that their biphasic regions were too small to observe and that the actual sequence was L to HPL to $Q_{Ia\bar{3}d}$ to H. Reexamination of their bicontinuous cubic samples has now revealed them to be $Q_{Ia\bar{3}d}$ [15], and our speculation about the HPL phase offers a sensible explanation regarding their unexpected L + H samples. Most other experimental results on these blends address the effect of changing the molecular weight of the homopolymer. We are currently exploring this along with the effects of changing the segregation.

We are grateful to F.S. Bates, M.M. Disko, D.A. Hajduk, and D.E. Sullivan for useful discussions. This work has been supported by NSF through Grant No. DMR 94-05101 to F.S. Bates.

-
- [1] J.M. Seddon, *Biochim. Biophys. Acta* **1031**, 1 (1990); J.M. Seddon, E.A. Bartle, and J. Mingins, *J. Phys. Condens. Matter* **2**, SA285 (1990).
 - [2] R. Lipowsky, *Nature (London)* **349**, 475 (1991).
 - [3] K. Larsson, *J. Phys. Chem.* **93**, 7304 (1989).
 - [4] D.C. Turner *et al.*, *J. Phys. II (France)* **2**, 2039 (1992).
 - [5] R. Strey *et al.*, *J. Chem. Soc. Faraday Trans.* **86**, 2253 (1990).
 - [6] R. Strey, *Colloid Polym. Sci.* **272**, 1005 (1994).
 - [7] M. Clerc, A.M. Levelut, and J.F. Sadoc, *J. Phys. II (France)* **1**, 1263 (1991); X. Auvray *et al.*, *Langmuir* **11**, 433 (1995).
 - [8] G.J.T. Tiddy *et al.*, *Langmuir* **11**, 390 (1995).
 - [9] S. Fischer *et al.*, *Liquid Crystals.* **17**, 855 (1994).
 - [10] F.S. Bates *et al.*, *Faraday Discuss.* (to be published).
 - [11] S. Förster *et al.*, *Macromolecules* **27**, 6922 (1994).
 - [12] G. Lindblom and L. Rilfors, *Biochim. Biophys. Acta* **988**, 221 (1989).
 - [13] D. Christensen, *Science News* **145**, 266 (1994).
 - [14] M.W. Matsen and M. Schick, *Phys. Rev. Lett.* **72**, 2660 (1994).
 - [15] D.A. Hajduk (private communication).
 - [16] D.J. Kinning *et al.*, *J. Chem. Phys.* **90**, 5806 (1989).
 - [17] K.I. Winey, E.L. Thomas, and L.J. Fetters, *J. Chem. Phys.* **95**, 9367 (1991).
 - [18] D.J. Kinning, K.I. Winey, and E.L. Thomas, *Macromolecules* **21**, 3502 (1988).
 - [19] K.I. Winey, E.L. Thomas, and L.J. Fetters, *Macromolecules* **25**, 422 (1992).
 - [20] M.M. Disko *et al.*, *Macromolecules* **26**, 2983 (1993).
 - [21] T. Hashimoto *et al.*, *Macromolecules* **25**, 1433 (1992).
 - [22] A.N. Semenov, *Macromolecules* **26**, 2273 (1993).
 - [23] L. Leibler and P.A. Pincus, *Macromolecules* **17**, 2922 (1984).
 - [24] M.D. Whitmore and J. Noolandi, *Macromolecules* **18**, 2486 (1985).
 - [25] E. Helfand, *J. Chem. Phys.* **62**, 999 (1975).
 - [26] K.M. Hong and J. Noolandi, *Macromolecules* **14**, 727 (1981).
 - [27] K.R. Shull, *Macromolecules* **26**, 2346 (1993).
 - [28] C.R. Kao and M. Olvera de la Cruz, *J. Chem. Phys.* **93**, 8284 (1990).